Study on the oxidation mechanism of micron- and nano-sized aluminum powders influenced by alumina shell

Yang Liu[1, a], Hui Ren[2, b, *]

1. The Civil-Military Integration Institute, China Center for Information Industry Development, Beijing 100091, China
2. The state key labortary of explosive science and technology, School of Machatronical Engineering, Beijing Institute of Technology, Beijing 100081, China
a. liuyang@ccidthinktank.com b. renhui@bit.edu.cn
***corresponding author**

Abstract: Thermal behaviors for aluminum particles at oxidative atmosphere gradually heating system were discussed. Heating micron- and nano-sized aluminum powders from room temperature to 1400℃ using thermal analysis method. The results showed that the reaction process for micron-sized aluminum particles can be divided into four stages which include the phase change of oxidized shell, increasing thickness of alumina shell, main broken shell oxidizing process and the phase change of alumina shell in high temperature. Thermal analysis for micro aluminum particles was carried out with shell thickness adjustments via ambient manual means. It turned out that the oxide layer thickness would have full limitation effects on the slow oxidation for micro aluminum particles with shell structure when it was increased above twice of the original thickness. The limitation effects of oxide shell thickness on the heating processes in gradually heating system were proposed. Humidity environment can make the thickness of alumina increase in a certain range when the particles are in nano-scale. Complete oxidation processes were observed but an increase of the oxidation temperature was identified.

Keywords: aluminum particles; core-shell structure; thickness of alumina shell; oxidation reaction; thermal analysis.

1. Introduction

Aluminum powder, as a combustible component in energetic materials such as propellants[2], explosives, and thermite[3], significantly enhances the performance of these materials[4]. Aluminum powder is a typical core-shell structure, consisting of an aluminum core and a uniformly dense alumina shell that encapsulates it[5]. The alumina layer, acting as a passivation layer under natural conditions, inhibits further oxidation of the aluminum in the core-shell structure. This also makes the process of aluminum oxidation under high-temperature conditions such as burning[6] relatively complex and difficult to directly analyze and observe. In recent years, the thermal reaction and combustion mechanisms of micron and nano-sized aluminum powders under different oxidation conditions have been a focus of research[7]. The study of the thermal reaction mechanisms of aluminum powders under special conditions can guide their application in energetic systems. Furthermore, metal powders at the micro and nano scale, particularly aluminum powders, have varying combustion and detonation conditions under different environments, and there has been no consistent conclusion regarding their reaction processes[8]. Existing reaction models each have their limitations, especially in accurately describing the changing patterns of particle size and oxide shell thickness during combustion, which is also a shortfall in the study of aluminum powder oxidation behavior.

This research explores the oxidation behavior of micron and nano-sized aluminum powders in oxidizing atmospheres, analyzing the oxidation mechanisms under slow heating. The thickness of the oxidation layer of aluminum powder increases with the diameter of the aluminum particles within a certain range. The oxidation layer thickness of micron and nano-sized aluminum powders increases to some extent during heat treatment compared to natural conditions. The oxide layer thickness of nano-sized aluminum powders treated with humidity also increases, and this study investigates the similarities and differences in the

oxidation reactions of aluminum particles with different alumina shell thicknesses, analyzing the impact of different particle sizes on the limiting effect of the oxidation layer on reaction activity.

2. Experimental

2.1. Sample Characterization

2.1.1. Morphological Analysis of Aluminum Powder Samples

The experimental samples were provided by Anshan Industrial Micron Aluminum Powder Co., Ltd. There were four micron-sized samples, numbered from Sample 1 to Sample 4 in order of increasing particle size. There were two nano-sized aluminum powders, Sample 5 and Sample 6. For a clearer and more direct understanding of the samples' appearances, a Hitachi S2700 Scanning Electron Microscope (SEM) and a FEI Company Tecnai G2 F30 Field Emission Transmission Electron Microscope (TEM) were used to characterize the micron and nano-sized aluminum powders, respectively. As shown in Figure 1, the surface of the micron-sized aluminum powder particles is smooth, without apparent defects or agglomeration, and has good sphericity. The nano-sized aluminum powders were dispersed in ethanol solution for observation, showing uniform particle size distribution, good sphericity, complete shapes, minimal agglomeration, clear core-shell structures, with an amorphous alumina outer layer and an aluminum core.

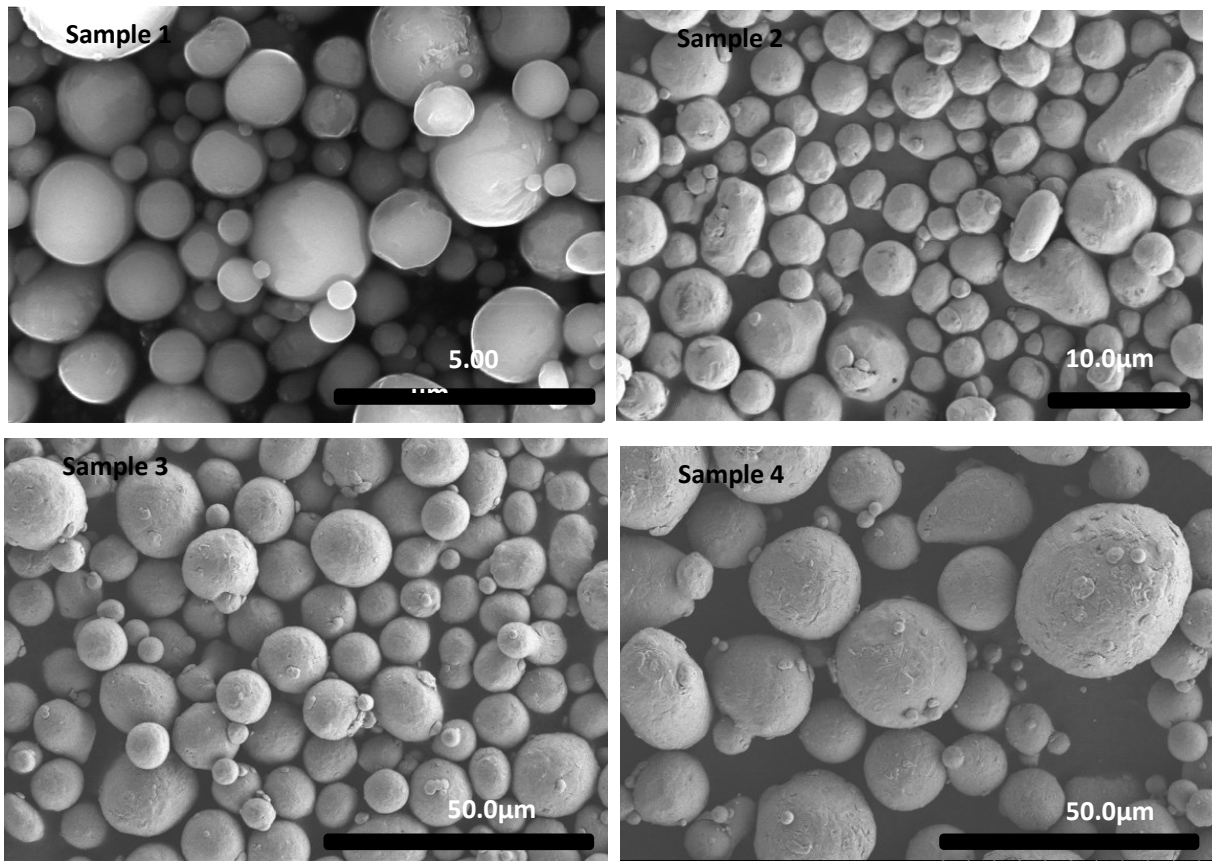

(1)

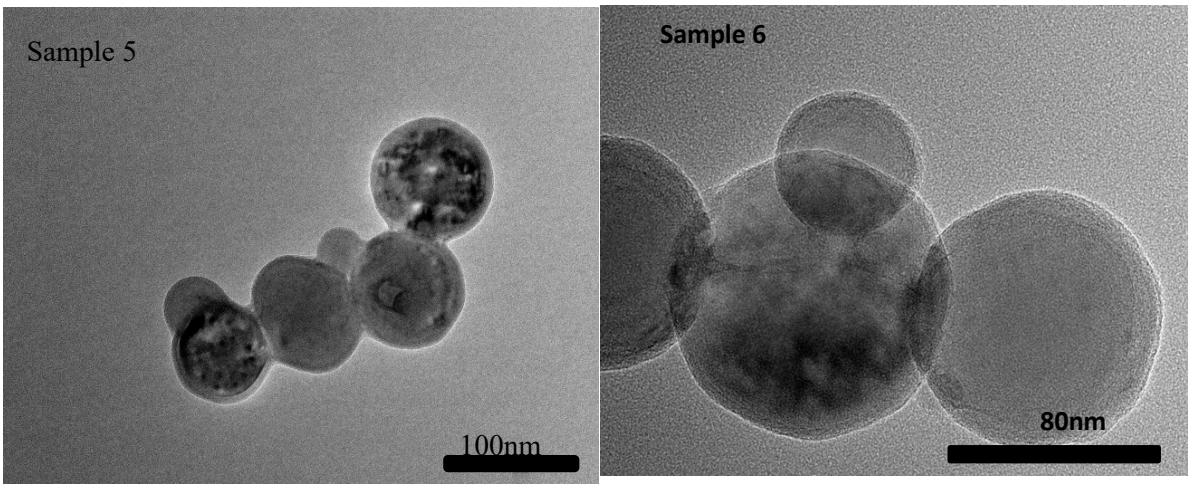

(2)

Figure 1 (1) SEM images of micron-sized aluminum powders; (2) TEM images of nano-sized aluminum powders.

2.1.2. Alumina Shell Thickness and Activity

The particle size distribution of the samples was measured using a Malvern Mastersizer 2000 laser particle size analyzer. Elemental and impurity contents were characterized using a glow discharge mass spectrometer, as impurities can affect the uniformity of the oxide layer, thereby altering the properties of the aluminum particle's oxidation layer. The core-shell structure and oxide layer thickness of nano-sized aluminum powder could be directly quantified through transmission electron microscopy. However, the oxide layer thickness of micron-sized aluminum powder could not be directly measured through methods such as scanning electron microscopy and had to be studied indirectly through parameters like the active aluminum content[9]. Calculations indicated that the average thickness of the alumina shell of the micron and nano-sized aluminum powders ranged from 2.9 to 13 nanometers, increasing with particle size[10]. The parameters of the samples are provided in Table 1.

Table 1 Properties of Aluminum Powders

Sample	D50	Thickness of Al_2O_3 shell	Active aluminum
1	2.51μm	2.9nm	98.16%
2	5.24μm	4.8nm	98.30%
3	13.35μm	8.1nm	98.67%
4	24.02μm	13.0nm	98.80%
5	60.15nm	2.4nm	72.02%
6	91.32nm	2.8nm	78.92%

2.2. Experimental Procedure

Differential Scanning Calorimetry - Thermogravimetric Analysis (TG-DSC), as a method that can precisely measure the mass and heat flow changes of samples during heating, has been widely used in studies of the thermal oxidation process of metal powders. In the experiments, TG-DSC was combined with other analytical methods such as Mass Spectrometry (MS), X-ray Diffraction (XRD), SEM, and TEM to control the reaction process, collect intermediate and final reaction products, and comprehensively analyze the entire oxidation process of the samples.

2.2.1. Thermal Analysis

The heating rate for the experiments was set at 20°C/min, with a heating range from room temperature to 1500°C. The sweep gas, which also served as the reaction atmosphere, was oxygen, flowing at a rate of 1.2L/h to ensure complete reaction of the aluminum powder with the gas while maintaining constant

pressure in the reaction environment. Before the experiments, samples and pre-treated alumina crucibles were placed in a vacuum oven and dried at 40°C for 24 hours. Approximately 2mg ± 0.3mg of the sample was evenly placed at the bottom of the alumina crucible in a dry environment. Before heating, the sample was purged with argon gas for five minutes to ensure no other oxidative gases interfered with the sample's reaction environment. To meet the accuracy and repeatability requirements of the experiment, thermal analysis of the same process was repeated three times for each sample. These repeated experiments also helped in real-time correction of the experimental procedure and guidance and adjustment of subsequent parameters.

2.2.2. Collection and Characterization of Intermediate Products

To clarify the specific reaction processes of each stage and more accurately analyze the oxidation mechanism, the full-range heating experiment was adjusted to terminate at different reaction temperature stages, and intermediate products were collected and characterized. The specific operation was to stop the heating program of the instrument at different temperatures, rapidly replacing the oxidative sweep gas with an inert protective gas after heating the sample to a specific temperature. Then the instrument's cooling program was initiated to cool the sample under an inert atmosphere back to room temperature. After the reaction, the intermediate product samples in the alumina crucible were collected for SEM and XRD characterization.

2.2.3. Oxide Layer Thickness Treatment

Under natural conditions, the oxide layer of micron-sized aluminum powder thickens with increasing particle size[11]. The properties of the oxide layer can be altered by heating treatment on the surface of the aluminum powder[12], and the limiting effect of changes in the thickness of the alumina layer before and after treatment on reactant diffusion was compared. The oxide layer thickness of micron-sized aluminum powder samples was increased through precise control in a thermal analyzer, changing the phase state and thickness of the surface alumina layer to achieve the goal of thickening the oxide layer of micron-sized aluminum powder samples. For the treated samples, the same thermal analysis study was conducted for comparison. Nano-sized aluminum powder is more sensitive to temperature changes. The alumina shell of nano-sized aluminum powder was thickened through humidity treatment, specifically by placing the nano-sized aluminum powder in a humid air environment (saturated vapor pressure) at 45°C for 72 hours. After the humidity treatment, the samples were thoroughly dried in a vacuum oven to remove the impact of surface moisture, followed by the same thermal analysis experiment to compare the effect of oxide layer thickness on the oxidation reaction.

3. Results and Discussion

3.1. Thermal Reaction Behavior of Aluminum Powder

3.1.1. Micron-sized Aluminum Powder

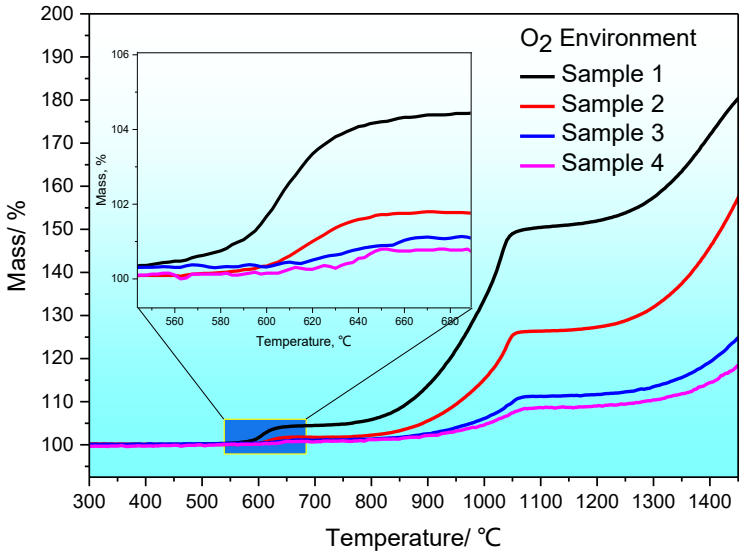

Fig.2 The TG curves of micron-sized aluminum powders

The thermogravimetric (TG) curves of micron-sized aluminum powders are shown in Figure 2. These powders exhibit two stages of weight gain during slow heating in an oxygen environment. Although the trend of weight gain is consistent across all four samples, the absolute values of weight gain differ due to varying particle sizes. The first stage of weight gain occurs at around 620°C (as shown in the magnified section of the figure), ranging between 1% and 4%, and decreases with increasing particle size. The second stage begins gradually at 850°C and continues until 1050°C, with the weight gain decreasing as particle size increases. This stage, where Sample 1 shows up to 80% weight gain, represents the main oxidation phase.

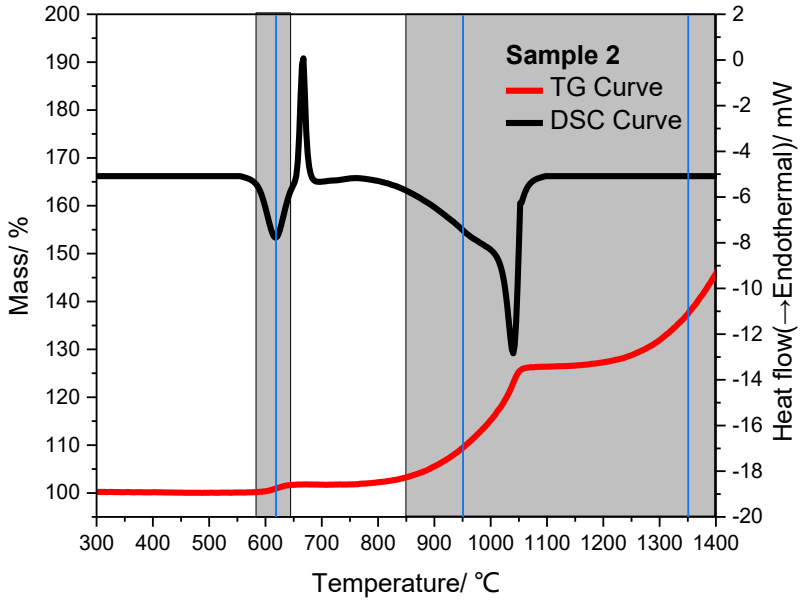

Fig.3 TG-DSC curves of sample 2

Figure 3 presents the TG-DSC curves of Sample 2, selected as a representative for analyzing the reaction mechanism of micron-sized aluminum powder. The corresponding exothermic and weight gain curves indicate the sample's exothermic-absorptive-exothermic process. The first exothermic peak corresponds to the weight gain during the initial oxidation reaction, the second absorptive peak occurs between 660°C-670°C, representing the melting process of aluminum, and the final exothermic peak signifies the intense oxidative reaction of the aluminum sample with the oxidizing gas. To further understand the changes at different reaction stages, the reaction was stopped at 620°C (end of the first stage of weight gain), 950°C (maximum rate of weight gain in the second stage), and 1350°C (end of the final stage of the reaction, as indicated by the blue line in Figure 3). Intermediate products were collected for SEM and XRD characterization.

At the 620°C temperature point, based on the TG-DSC curves, only a small portion of aluminum is oxidized. The XRD pattern (Figure 4) shows the presence of γ-Al2O3, indicating a phase transition in the alumina shell from its initial amorphous state to γ-Al2O3. Eventually, as the temperature exceeds 1050°C, the reaction slows down, and the sample's weight gain decreases. During this high-temperature stage, the oxidation reaction continues, leading to a phase transition in alumina, ultimately forming the most stable α-Al2O3. This phase transition of alumina aligns with the temperatures reported in the literature[13].

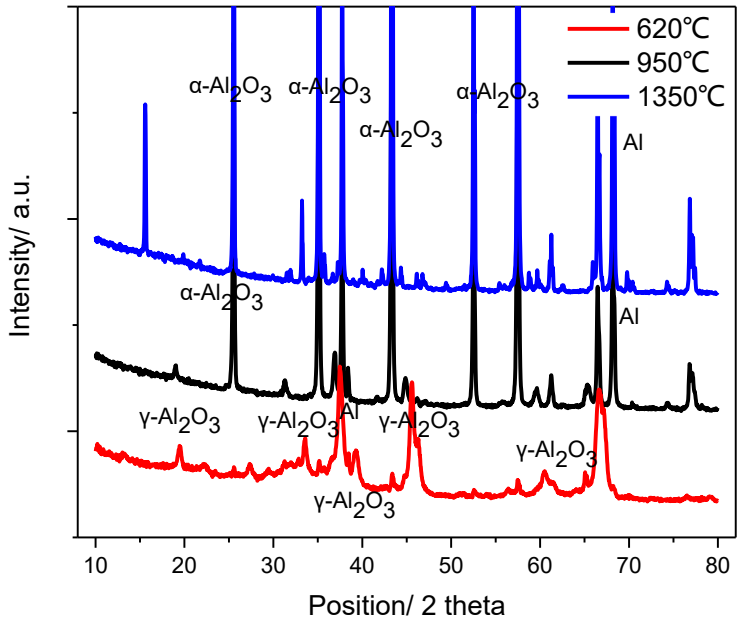

Fig.4 XRD pattern of intermediate products at different temperatures of sample 2

The SEM images (Figure 5) of the intermediate products of Sample 2 reveal that at 620°C, the samples still maintain their spherical shape. However, above the melting point of aluminum, hollow shell structures and broken alumina fragments are observed, with the thickness of the alumina shell exceeding the original thickness. The thermal expansion coefficients of alumina and aluminum differ, with the latter being approximately ten times that of the former. During heating, the expansion and phase change of the aluminum core exert pressure on the alumina shell. The melting process intensifies the expansion, and the alumina shell cracks at weak points or defects under internal pressure. These cracks form channels, allowing oxidizing gases to enter the shell and react with the molten aluminum core. The relatively loose crystal structure of γ-Al2O3 facilitates the reaction of atmospheric oxygen with the internal liquid aluminum at the interface, resulting in the formation of alumina and the weight gain observed in the second stage. At 1350°C, the samples still display hollow spherical structures with some deformation and particle agglomeration.

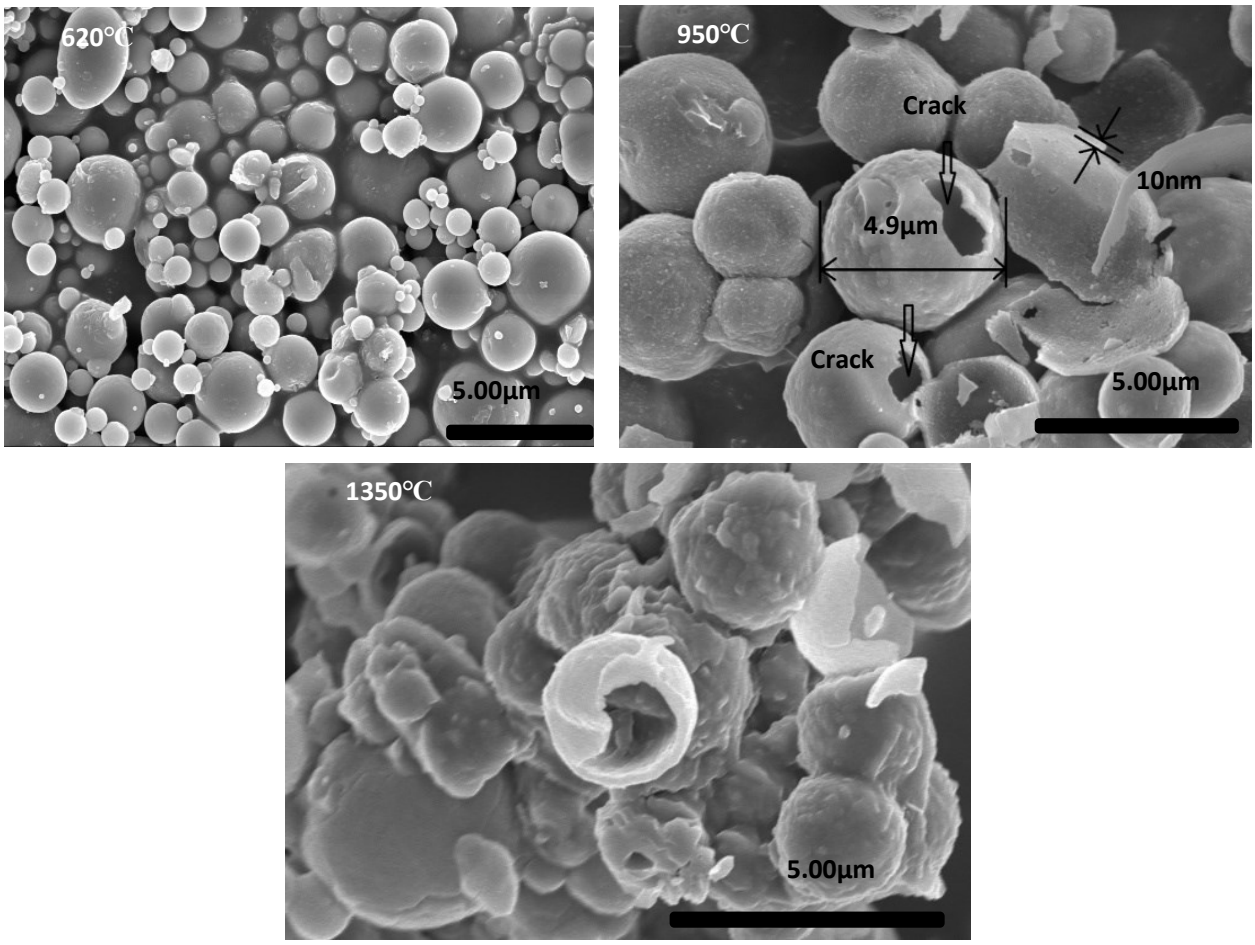

Fig.5 SEM images of intermediate products at different temperatures of sample 2

3.1.2. Nano-sized Aluminum Powder

The TG-DSC analysis of nano-sized samples, as shown in Figure 6, reveals that nano-sized aluminum powder reacts vigorously at around 540°C. Due to the size effect of nano-particles, the melting point of the metal is reduced, and thus a violent reaction occurs below the melting point of aluminum[8b]. The sample releases a significant amount of heat and reaches its maximum weight gain. After 950°C, the sample's mass increases slightly, but no heat is released. Due to potential instrument errors at high temperatures, the minor weight gain in this stage is attributed to the phase transformation of the aluminum powder at high temperatures. The nano-sized aluminum powder undergoes rapid weight gain under slow heating conditions, and the reaction products are black-gray solid residues, indicating combustion of the nano-sized aluminum powder at 540°C. The reaction rate of the samples is consistent, and the entire process is diffusion-controlled, with the onset temperature slightly increasing with particle size, likely due to the thicker oxide layer of larger nano-sized aluminum particles.

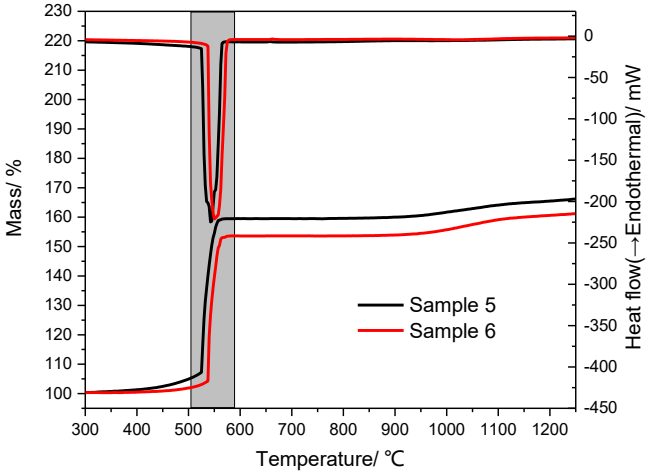

Fig.6 TG-DSC curves of nano-sized aluminum powders in oxygen

3.2. Study on the Thickening of the Oxide Shell of Micron-sized Aluminum Powder

The TG curves of the thermal reaction behavior of micron-sized aluminum powder reveal that smaller particle samples react more thoroughly, while larger particles only partially oxidize. SEM images of the final products after thermal reactions of different particle sizes (Figure 7) show that the oxidation layer of smaller particle samples breaks more completely. Larger particle samples still maintain a certain spherical structure, with some unreacted active aluminum inside. The external oxide layer structure can still protect the internal aluminum powder from oxidizing with the external environment at high temperatures.

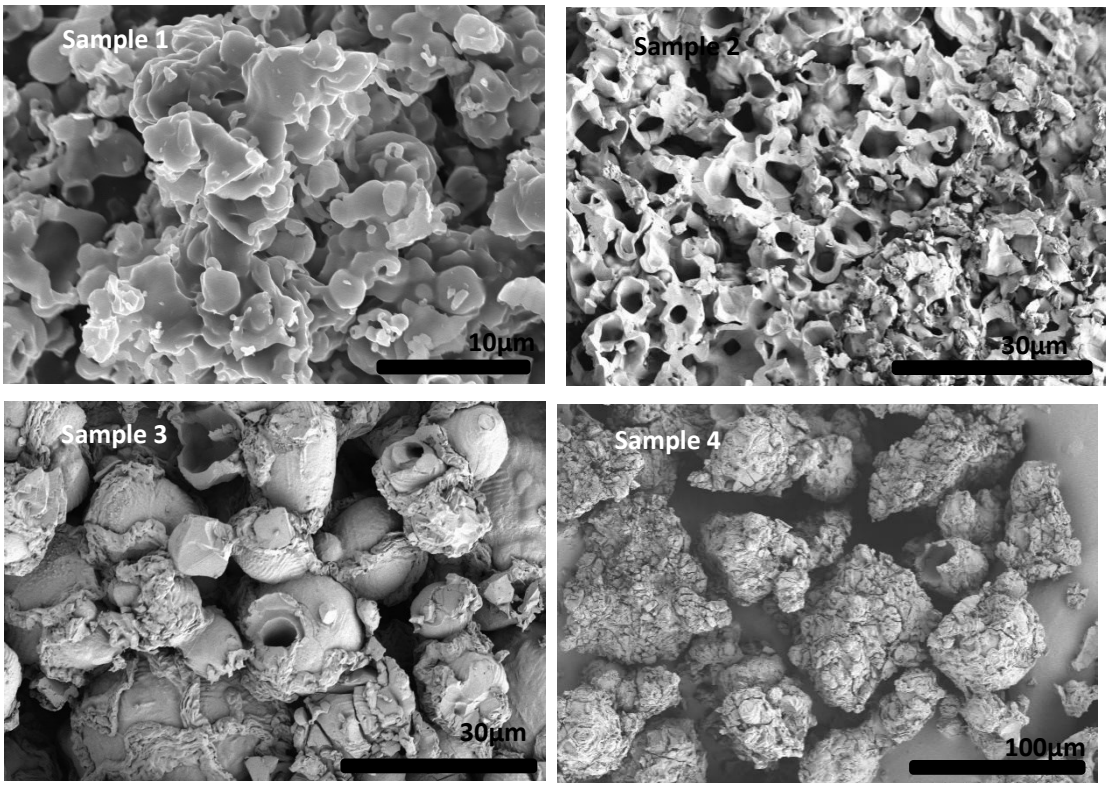

Fig.7 SEM images of final products after micron-sized aluminum samples being heated in the whole temperature scale

The first weight gain process of the aluminum powder is due to the increase in thickness of the oxidation layer, while the second weight gain process is due to shell-breaking oxidation reactions. According to the experimental results, the samples were heated to 620°C for oxidation layer thickening treatment, which means the original samples were heated to 620°C and then cooled to room temperature under an inert atmosphere. Sample 2 was used as an example, and the treated sample was designated as 2*. Figure 8 shows the TG-DSC curve comparison. The weight gain of Sample 2*, which underwent oxidation layer thickening treatment, was greatly limited. When heated to a high temperature of 1400°C, the weight gain was less than 13%, originating from smaller components such as sub-micron particles in the sample. The DSC curve shows that after the treatment, the reaction of the aluminum powder was significantly restricted. Apart from a distinct endothermic peak at 660°C, the melting point of aluminum, there were no significant changes in the entire reheating exothermic curve, with the exothermic peaks around 620°C and between 850°C-980°C completely disappearing. This suggests that aluminum did not undergo intense oxidative reactions with the oxidizing gases in the environment.

The change in thickness of the oxidation layer was calculated based on the weight gain in the first stage of the sample, assuming:

1. The reaction interface is the inside of the spherical shell oxidation layer.
2. The reaction products are all alumina, uniformly attached to the inside of the oxidation layer.
3. The spherical shell is rigid and does not deform during heating.

Based on the reaction equations, equations (1) and (2) were derived, where W is the original mass of the sample particle, R_1 is the original diameter of the sample, R_2 is the inner diameter of the alumina shell, R_3 is the inner diameter of the alumina shell after the end of the first stage reaction, m is the weight gain obtained from the TG curve, ρ_1 is the density of aluminum, and ρ_2 is the density of alumina.

$$mW = \frac{24}{51} \cdot \frac{4}{3}\pi(R_2^3 - R_3^3)\rho_2 \quad (1)$$

$$W = \frac{4}{3}\pi(R_1^3 - R_2^3)\rho_2 + \frac{4}{3}\pi R_2^3\rho_1 \quad (2)$$

The thickness of the oxidation layer of untreated samples was already known [7g]. According to the formula, the thickness of the oxidation layer before the first stage of heating (δ_1) and after heating at 620°C in the first stage (δ_2) was calculated $\delta_1 \approx \delta_2$. The thickness of the oxidation layer after the thickening treatment was twice that of the original thickness of the untreated samples. When the thickness of the oxidation layer of micron-sized aluminum powder exceeds twice its original thickness, it can restrict the oxidation reaction and prevent it from occurring.

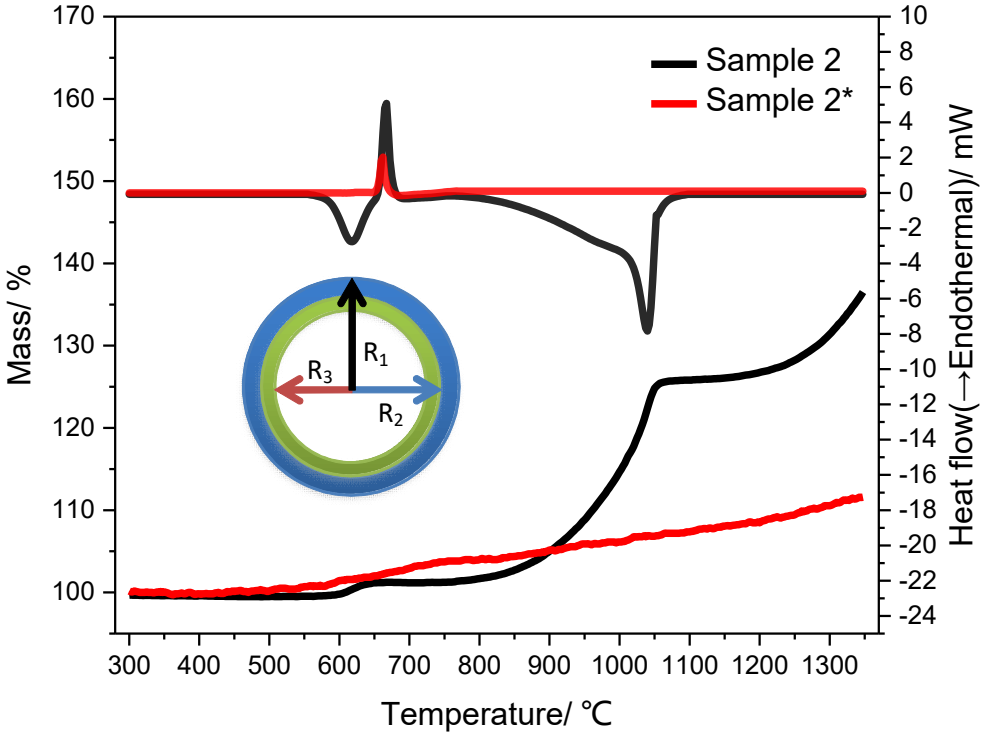

Figure 8: Comparison of TG-DSC curves between original sample 2 and sample 2 with a thicker alumina shell*

3.3. Study on the Thickening of the Oxide Layer of Nano-sized Aluminum Powder

3.3.1. Thickness of the Oxide Layer of Nano-sized Aluminum Powder

The oxidation process of nano-sized aluminum powder in an oxygen environment is faster compared to micron-sized aluminum powder, and it is difficult to thicken the alumina shell layer through heating. Therefore, the alumina shell of nano-sized aluminum powder was thickened in a humidity environment. The partial TEM images of samples 5* and 6* after humidity treatment are shown in Figure 9. The measurement of the average thickness of the oxide layer of nano-particle samples before and after treatment shows that the humidity environment can thicken the oxide layer of nano-sized aluminum powder, increasing the original thickness by more than 90%.

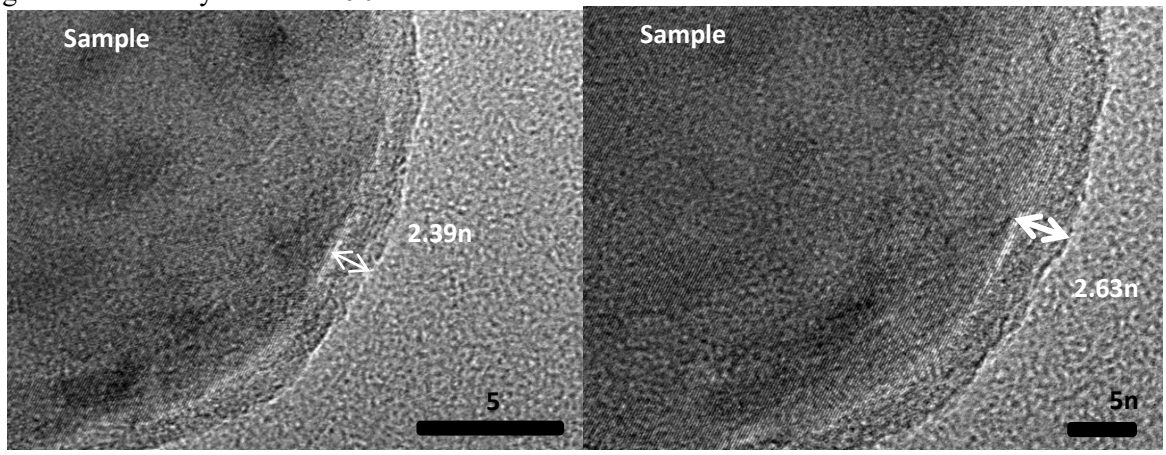

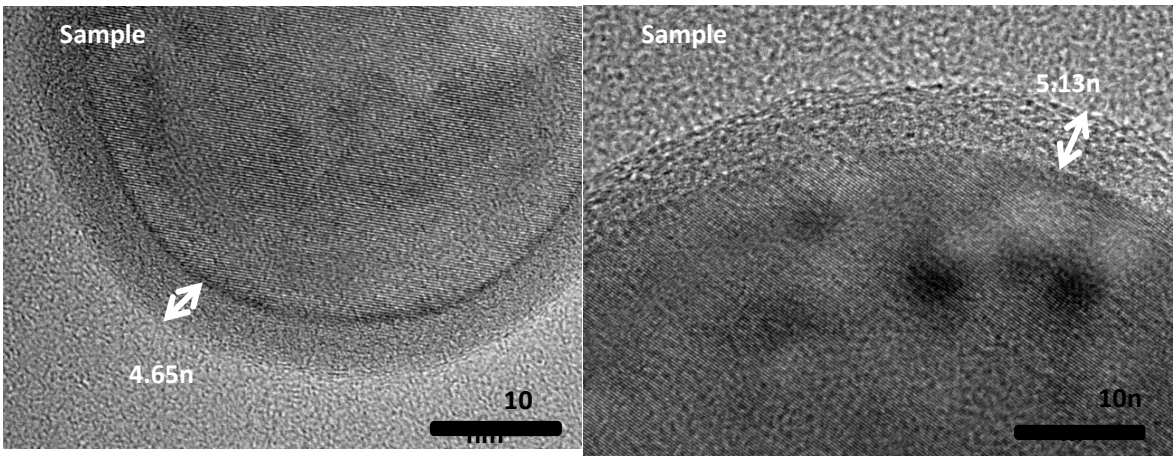

Fig.9 Comparison TEM images of nano-sized aluminum samples between sample 5, 6 and sample 5*, 6*

3.3.2. Oxidation Behavior of Nano-sized Aluminum Powder

The thermal analysis characterization of the treated samples, as shown in Figure 10, indicates that the increase in the thickness of the oxide layer raises the reaction temperature of the samples, but does not limit the reaction, allowing the samples to fully react and oxidize completely. Therefore, for nano-sized aluminum powder, when the oxide layer thickness is less than 5.3nm, it does not significantly limit the oxidation reaction of the aluminum powder.

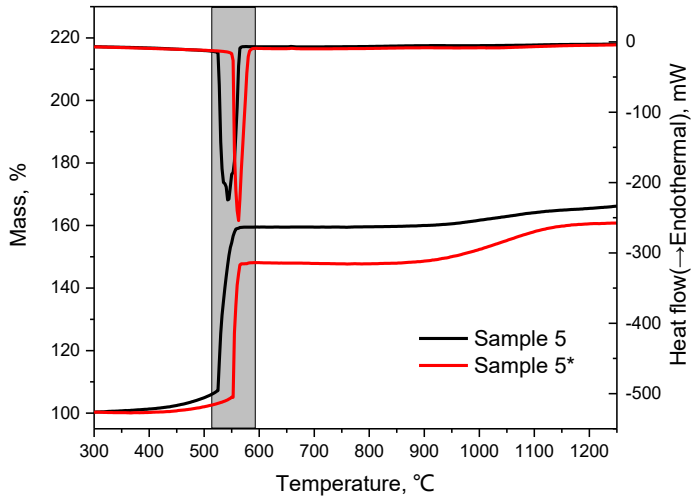

Fig.10 Comparison of TG-DSC curves between aluminum sample 5 and sample 5*

4. Conclusion

The reaction of micron-sized aluminum powder is divided into four stages: thickening and phase transition of the oxide layer; melting of the aluminum core; intense oxidation reaction of the aluminum powder; high-temperature phase transition of alumina. Nano-sized aluminum powder combusts under slow heating, occurring around 550°C, with the temperature slightly increasing as the sample particle size increases.

The thickness of the oxide layer of micron-sized aluminum powder can be achieved through heating. Calculations show that after the first stage of the reaction, the thickness of the oxide layer of micron-sized aluminum powder becomes twice that of the original sample. The aluminum particles with the altered oxide shell thickness due to heat treatment significantly limit the slow heating oxidation reaction. For nano-sized

aluminum powder, the humidity environment has a certain oxidizing effect on the thickness of the oxide layer, increasing the original thickness by 50%-60%, but it does not limit the combustion of the nano-sized aluminum powder, only slightly increasing the reaction temperature.

5. Reference

[1] a) E. L. Dreizin and M. Schoenitz, "Progress in Energy and Combustion Science" 2015, 50, 81-105; b) A. M. Starik, A. M. Savel'ev and N. S. Titova, "Combustion, Explosion, and Shock Waves" 2015, 51, 197-222; c) D. S. Sundaram, V. Yang and V. E. Zarko, "Combustion, Explosion, and Shock Waves" 2015, 51, 173-196.

[2] F. Maggi, S. Dossi, C. Paravan, L. T. Deluca and M. Liljedahl, "Powder Technology" 2015, 270, 46-52.

[3] Zheng Guoqiang, Zhang Wenchao, Xu Xing, Shen Ruiqi, Deng Jiping, and Ye Yinghua, "Journal of Inorganic Materials" 2015, Vol. 30, 610–614.

[4] a) An Ting, Zhao Fengqi, Yi Jianhua, Fan Xuezong, Gao Hongxu, Hao Haixia, Wang Xiaohong, Hu Rongzu and Pei Qing, "Acta Physico-Chimica Sinica" 2011, 27, 281-288; b) Zhu Yanli, Jiao Qingjie, Huang Hao and Ren Hui, "Chemical Journal of Chinese Universities" 2013, 34, 662-667; c) Zeng Liang, Jiao Qingjie, Ren Hui and Zhou Qing, "Chinese Journal of Explosives & Propellants (Huozhayao Xuebao)" 2011, 34, 26-29.

[5] a) V. Yang, D. Sundaram and P. Purl, "Proceedings of 2010"; b) Y. S. Kwon, A. A. Gromov, A. P. Ilyin and G. H. Rim, "Applied Surface Science" 2003, 211, 57-67.

[6] G. A. Risha, S. F. Son, R. Yetter, V. Yang and B. Tappan, "Proceedings of the Combustion Institute" 2007, 31, 2029-2036.

[7] a) X. Zhu, M. Schoenitz and E. L. Dreizin, "The Journal of Physical Chemistry C" 2009, 113, 6768-6773; b) C. Badiola, R. J. Gill and E. L. Dreizin, "Combustion and Flame" 2011, 158, 2064-2070; c) T. R. Sippel, T. L. Pourpoint and S. F. Son, "Propellants, Explosives, Pyrotechnics" 2013, 38, 56-66; d) G. A. Risha, J. L. Sabourin, V. Yang, R. A. Yetter, S. F. Son and B. C. Tappan, "Combustion Science and Technology" 2008, 180, 2127-2142; e) S. Rossi, E. L. Dreizin and C. K. Law, "Combustion Science and Technology" 2001, 164, 209-237; f) L. Ernst, F. Dryer, R. Yetter, T. Parr and D. Hanson-Parr, "Proceedings of the Combustion Institute" 2000, 28, 871-878; g) Y. Gan and L. Qiao, "Combustion and Flame" 2011, 158, 354-368.

[8] a) Cheng Zhipeng, Yang Yi, Wang Yi, Li Miaomiao and Li Fengsheng, "Acta Physico-Chimica Sinica" 2008, 23, 152-156; b) C. Kong, D. Yu, Q. Yao and S. Li, "Combustion and Flame" 2016, 165, 11-20.

[9] Zeng Liang in "Study on the Influence of Core-Shell Structure Aluminum Powder on the Reaction Process of Aluminized Explosives," Beijing Institute of Technology, 2011.

[10] Zeng Liang, Jiao Qingjie, Ren Hui and Zhou Qing, "Journal of Beijing Institute of Technology" 2012, 2, 020.

[11] B. Rufino, F. Boulc'h, M.-V. Coulet, G. Lacroix and R. Denoyel, "Acta Materialia" 2007, 55, 2815-2827.

[12] a) Wang Zhiyong, Peng Chaoqun, Wang Richu, Wang Xiaofeng and Liu Bing, "Journal of Inorganic Materials" 2013, 28, 171-176; b) Lu Yuan, Li Jinglong, Yang Jianfeng and Li Peng, "Journal of Inorganic Materials" 2015, 30, 277-281.

[13] Li Jiguang, Sun Xudong, Zhang Min, Li Xiaodong and Ru Hongqiang, "Journal of Inorganic Materials" 1998, 803-807.